

Model-Predictive Flux Control of Induction Motor Drives With Switching Instant Optimization

Yongchang Zhang, *Member, IEEE*, and Haitao Yang, *Student Member, IEEE*

Abstract—Conventional model-predictive torque control (MPTC) requires tedious and time-consuming tuning work for stator flux weighting factor, and presents relatively high torque ripples. To solve these problems, this paper proposes a model-predictive flux control (MPFC) for two-level inverter-fed induction motor (IM) drives. The references of stator flux magnitude and torque in conventional MPTC are converted into an equivalent reference of stator flux vector in the proposed MPFC. As only the tracking error of stator flux vector is required in the cost function, the use of weighting factor is eliminated. The optimal voltage vector is selected based on the principle of stator flux error minimization and its switching instant is optimized rather than being in the beginning of each control period. The proposed MPFC with and without switching instant optimization are both implemented in a 32-bit floating digital signal processor, and they are compared in detail in terms of torque ripple, current harmonics, and average switching frequency. Both digital simulations and experimental tests were carried out on a two-level inverter-fed IM drive, and the obtained results validate the effectiveness of the proposed method.

Index Terms—Induction motor (IM) drives, model-predictive flux control (MPFC), torque control, weighting factor.

I. INTRODUCTION

FOR HIGH-PERFORMANCE control of induction motor (IM) drives, field-oriented control (FOC) and direct torque control (DTC) are two well-established methods [1]–[3]. In FOC, the stator currents are decomposed into torque component and flux component in synchronous frame, and they are regulated separately using proportional-integral (PI) controllers. A modulation block is subsequently utilized to generate the final gating pulses. Good performance of torque and flux control can be achieved, but it requires fine tuning work for the inner current loops [4]. In DTC, a voltage vector is directly selected based on a predefined switching table and two hysteresis comparators. It features very quick dynamic response and simple structure, but exhibits high steady-state torque ripple and variable switching frequency [2], [3], [5].

Recently, model-predictive torque control (MPTC) has gained increasing attention in both academic and industrial communities due to its intuitive concept, high flexibility, and easy

Manuscript received November 19, 2014; revised March 3, 2015; accepted April 14, 2015. This work was supported in part by the National Natural Science Foundation of China under Grant 51207003 and Grant 51347004, and in part by the Beijing Nova Program under Grant xx2013001. Paper no. TEC-00774-2014.

The authors are with the Power Electronics and Motor Drives Engineering Research Center of Beijing, North China University of Technology, Beijing 100144, China, and also with the Collaborative Innovation Center of Electric Vehicles in Beijing, Beijing 100084, China (e-mail: yozhang@ieee.org; yht-seaky@gmail.com).

Color versions of one or more of the figures in this paper are available online at <http://ieeexplore.ieee.org>.

Digital Object Identifier 10.1109/TEC.2015.2423692

incorporation of constraints [6], [7]. The development of powerful and fast microprocessors makes MPTC a reality in the control of IM drives, and it has been considered as an effective alternative to conventional FOC and DTC [6], [8]–[12]. In MPTC, the evolutions of torque and stator flux are predicted based on system model, and they are evaluated to obtain optimal output of the controller according to a predefined optimization criterion [7]. A high-bandwidth explicit model-predictive controller in [11] is developed, exhibiting high dynamic performance at various operating points. In [12], a hysteresis-based MPTC is investigated for the control of a three-level inverter-fed IM drive, reducing the average switching frequency up to 50% compared to that of standard DTC. To obtain accurate prediction of the state variable, a precise discrete-time model with time-varying components is developed in [6], and a cost function consists of torque and stator flux error is evaluated to determine the optimal voltage vector.

In spite of the intuitive concept and quick response featured by MPTC, as the control variables of torque and stator flux have different units and amplitudes, a proper weighting factor for stator flux must be designed in order to achieve satisfactory performance [6]–[9]. Unfortunately, currently, the tuning of weighting factor is still an open problem, and mostly, it is designed based on empirical procedures, which is time-consuming and tedious. To cope with this problem, several methods have been proposed, including multiobjective optimization based on a ranking approach [8], optimizing weighting factor based on minimization of torque ripple [9], fuzzy decision-making strategy [13], etc. Although these schemes are effective in tackling with the problem of weighting factor tuning, they are usually complicated. In two-level inverter-fed IM drives, the control problems are usually formulated only for two control variables, namely torque and flux. Hence, it is possible to eliminate the use of weighting factor by investigating the inherent relationship between torque and stator flux, which should be simpler than prior methods [8], [9], [13].

In conventional MPTC, only one voltage vector is selected and it is not applied until the next control period due to the updating mechanism of modern microprocessors. The single-vector-based MPTC poses some limitations on the achievable performance. To obtain better steady-state performance, recently, the concept of duty cycle control was introduced in MPTC by dividing the control period into two intervals: one for the nonzero vector selected from MPTC and another for an appropriate zero vector [9], [14]. This method produces two changes of voltage vectors: one at the beginning of control period and the other at the instant of applying zero vector, resulting significant increase in the switching frequency. In fact, if we take the instant applying the selected voltage vector as an extra freedom, it is still

possible to improve the steady state performance [15], but the vector change at the beginning of control period can be abolished, hence not increasing the average switching frequency too much. As both torque and stator flux are used in the cost function, the method in [15] still suffers from the weighting factor tuning for stator flux.

To eliminate the weighting factor in conventional MPTC, this paper proposes a model-predictive flux control (MPFC) which translates the references of torque and stator flux into an equivalent new stator flux vector. As both components of this new flux vector have the same unit, it is evident that the weighting factor is no longer required; hence, the design procedure of MPFC in real applications is much simpler than that of MPTC [6]. Various methods have been proposed to achieve stator flux tracking, such as [16], [17], where the flux error is compensated in real time by modifying the precalculated switching instants of the optimal synchronous pulse pattern. The methods in [16] and [17] are very complicated and computational intensive, and they are mainly developed for high-power drives operating at very low switching frequency. In this paper, the proposed MPFC is mainly developed for low and medium two-level IM drives with relatively low control complexity. Two variants of MPFC are investigated in this paper. In the first variant, only one voltage vector is applied during one control period, while in the second variant, the freedom of switching instant of the selected voltage vector is employed to achieve better steady-state performance. Different from the scheme proposed in [15], which optimizes the switching instant and vector selection based on the principle of torque ripple minimization and stills requires the weighing factor for stator flux, the proposed MPFC tries to minimizing the tracking error of stator flux vector. As the new stator flux reference is equivalently converted from both torque and stator flux references, accurate and fast torque control can still be ensured while eliminating the use of weighting factors. The effectiveness of the proposed method is confirmed by experimental tests carried out on two-level inverter-fed IM drives.

II. DYNAMIC MODEL OF IM

By choosing stator flux ψ_s and stator current i_s as state variables, the model of IM can be expressed in stationary frame using complex vectors as [14], [18]

$$\dot{\mathbf{x}} = \mathbf{A}\mathbf{x} + \mathbf{B}\mathbf{u} \quad (1)$$

where $\mathbf{x} = [i_s \ \psi_s]^T$ are state variables, $\mathbf{u} = \mathbf{u}_s$ is the stator voltage vector, and

$$\mathbf{A} = \begin{bmatrix} -\lambda(R_s L_r + R_r L_s) + j\omega_r & \lambda(R_r - jL_r \omega_r) \\ -R_s & 0 \end{bmatrix} \quad (2)$$

$$\mathbf{B} = \begin{bmatrix} \lambda L_r \\ 1 \end{bmatrix}. \quad (3)$$

R_s , R_r , L_s , L_r , and L_m are the stator resistance, rotor resistance, stator inductance, rotor inductance, and mutual inductance, respectively, ω_r is electrical rotor speed, and $\lambda = 1/(L_s L_r - L_m^2)$.

The value of stator current and stator flux at the next control instant can be predicted using (1). The most simple and popular

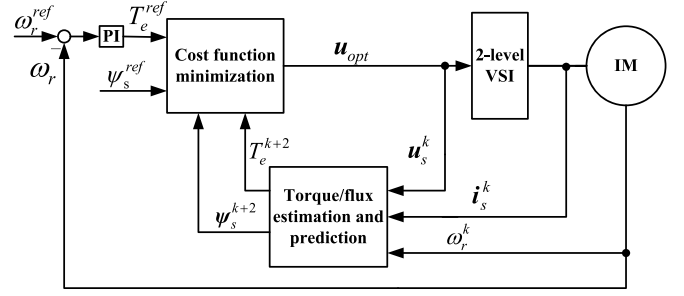


Fig. 1. Control diagram of the conventional MPTC.

method to discretize (1) is the first-order Euler method. However, its accuracy is relatively limited [19]. To achieve higher accuracy, the Cayley–Hamilton theorem is utilized in [6] to calculate the matrix exponential, which is computational intensive and complicated. In this paper, to achieve accurate prediction of stator current and stator flux while not increasing the computational burden too much, second-order Euler discretization is selected to discretize (1), which is expressed as [14], [20]

$$\begin{cases} \mathbf{x}_p^{k+1} = \mathbf{x}^k + T_{sc} (\mathbf{A}\mathbf{x}^k + \mathbf{B}\mathbf{u}_s^k) \\ \mathbf{x}^{k+1} = \mathbf{x}_p^{k+1} + \frac{T_{sc}}{2} \mathbf{A} (\mathbf{x}_p^{k+1} - \mathbf{x}^k) \end{cases} \quad (4)$$

where T_{sc} is the control period, \mathbf{x}_p^{k+1} is the predictor-corrector of state vector, and $\mathbf{x}^{k+1} = [i_s^{k+1} \ \psi_s^{k+1}]^T$ is predicted state vector for stator current and stator flux.

The electromagnetic torque T_e can be predicted as

$$T_e^{k+1} = \frac{3}{2} N_p \psi_s^{k+1} \otimes i_s^{k+1} \quad (5)$$

where N_p is the number of pole pairs and \otimes represents the cross product.

III. CONVENTIONAL MPTC

Based on the system model, the standard MPTC scheme predicts electromagnetic torque and stator flux for all feasible voltage vectors provided by an inverter, and then, the best one is determined by minimizing a cost function, which consists of torque and flux tracking error. The diagram of MPTC considering one-step delay compensation [6], [14] is shown in Fig. 1, where an external PI speed controller is employed to generate the torque reference.

A. State Estimation

Accurate state estimation is a key factor for ensuring good performance of MPTC in real-time implementation. A full-order observer for the flux and torque estimation is adopted due to its accuracy and insensitivity to parameter variation over a wide speed range. The mathematical model of the observer is shown as follows:

$$\frac{d\hat{\mathbf{x}}}{dt} = \mathbf{A}\hat{\mathbf{x}} + \mathbf{B}\mathbf{u} + \mathbf{G} (i_s - \hat{i}_s) \quad (6)$$

where $\hat{\mathbf{x}} = [\hat{i}_s \ \hat{\psi}_s]^T$ is the estimated state for stator current and stator flux.

A constant gain matrix G is employed in this paper to improve the stability of the observer, and it is expressed as [2]

$$G = - \begin{bmatrix} 2b \\ b/(\lambda L_r) \end{bmatrix} \quad (7)$$

where b is a negative constant gain. By using the gain matrix in (7), the real part of observer poles will be shifted to the left in the complex plane compared to the poles of IM, while the imaginary part of poles not changed much. This pole placement method can improve the convergence and stability of observer, especially at high speed, as shown in [2]. The selection of b is a compromise between the convergence speed and the noise immunity. A bigger b results in faster converge speed, but the observer is more sensitive to the noise. In this paper, b is chosen as -40 . The characteristic of the observer can be found in [21], and our previous work [2] has verified that the observer presents good accuracy over a wide speed range.

B. Vector Selection

Knowing the measured stator current i_s^k and estimated stator flux $\hat{\psi}_s^k$ from (6), the value of stator current and stator flux at the $(k+1)$ th instant can be obtained from (4) for a given stator voltage vector u_s^k . The predicted stator flux ψ_s^{k+1} and electromagnetic torque T_e^{k+1} from (5) are evaluated using a cost function J , which is expressed as a linear combination of torque and stator flux errors:

$$J = |T_e^{\text{ref}} - T_e^{k+1}| + k_\psi \left| |\psi_s^{\text{ref}}| - |\psi_s^{k+1}| \right| \quad (8)$$

where k_ψ is the weighting factor for stator flux. In conventional MPTC, the tuning of k_ψ is a nontrivial process. As shown in [9], the weighting factor of stator flux is optimized in real time to obtain the minimal torque ripple. The significant variations of the weighting factor indicate that the optimal weighting factor is dependent on the operating point and machine parameters and cannot be obtained directly through offline tuning.

In real-time implementation, one-step delay between the commanding voltage and the real voltage caused by digital processing will deteriorate the performance of MPTC [6], [22], [23]. To compensate this delay, the variables at $(k+2)$ th instant should be predicted for the evaluation of the cost function rather than $(k+1)$ th instant. A model-based prediction is adopted to diminish the influence of the time delay. First, the prediction of i_s^{k+1} and ψ_s^{k+1} is obtained according to (4). Second, i_s^{k+1} and ψ_s^{k+1} are used as initial value for the prediction of ψ_s^{k+2} and T_e^{k+2} ; thus, the final cost function J with the consideration of one step delay can be rewritten from (8) to (9) as

$$J = |T_e^{\text{ref}} - T_e^{k+2}| + k_\psi \left| |\psi_s^{\text{ref}}| - |\psi_s^{k+2}| \right|. \quad (9)$$

For two-level inverter-fed IM drives, there are seven different voltage vectors, $u_{0(7)}, u_1, u_2, \dots, u_6$, as shown in Fig. 2. After the cost function J is evaluated for each voltage vector, the best one minimizing J is selected and applied in the next control period.

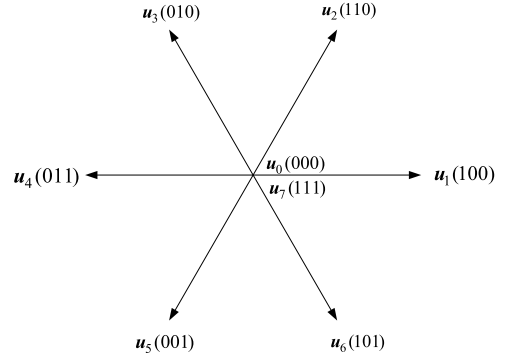


Fig. 2. Voltage vectors and corresponding switching states of the two-level inverter.

IV. PROPOSED MPFC

A. Principle of Basic MPFC

As torque and stator flux errors are combined into a single cost function in conventional MPTC, a proper weighing factor for stator flux is necessary to achieve simultaneous control of torque and stator flux. However, the lack of theoretical design method for weighting factors leads to a nontrivial tuning work [8]. In this section, a new stator flux vector reference is constructed based on the model of IM, which is equivalent to the original reference of torque and stator flux. As a result, the weighing factor is eliminated in the proposed MPFC.

The magnitude of stator flux vector reference ψ_s^{ref} is set to the rated value ψ_s^{ref} in this paper when the rotor speed is below based speed, namely

$$|\psi_s^{\text{ref}}| = \psi_s^{\text{ref}}. \quad (10)$$

The torque can be expressed as a cross product of stator flux and rotor flux, which is expressed as [2]

$$T_e = \frac{3}{2} N_p \lambda L_m (\psi_r \otimes \psi_s). \quad (11)$$

According to (11), if the rotor flux ψ_r is already known, the references of T_e^{ref} and ψ_s^{ref} should satisfy the following equation:

$$T_e^{\text{ref}} = \frac{3}{2} N_p \lambda L_m (\psi_r \otimes \psi_s^{\text{ref}}). \quad (12)$$

Based on (10) and (12), the stator flux vector reference ψ_s^{ref} can be expressed by ψ_s^{ref} and T_e^{ref} as

$$\psi_s^{\text{ref}} = \psi_s^{\text{ref}} \cdot \exp(j \cdot \angle \psi_s^{\text{ref}}) \quad (13)$$

$$\angle \psi_s^{\text{ref}} = \angle \psi_r + \arcsin \left(\frac{T_e^{\text{ref}}}{\frac{3}{2} p \lambda L_m |\psi_r| |\psi_s^{\text{ref}}|} \right). \quad (14)$$

Similar to the delay compensation in MPTC, the stator flux vector reference ψ_s^{ref} at $(k+2)$ th instant should be determined. However, this needs the information of T_e^{ref} and ψ_r at $(k+2)$ th instant. In general, the future reference of torque can be considered approximately equal to the present value of the reference, if the sampling frequency is much higher than the bandwidth of outer speed control loop [7]. For ψ_r at $(k+2)$ th instant, it can be predicted using the following procedure. The rotor flux ψ_r^{k+1}

can be obtained from $(k + 1)$ th stator flux and stator current as

$$\psi_r^{k+1} = \frac{L_r}{L_m} \psi_s^{k+1} - \frac{1}{\lambda L_m} i_s^{k+1} \quad (15)$$

where ψ_s^{k+1} and i_s^{k+1} are predicted from (4). After ψ_r^{k+1} is obtained from (15), the $(k + 2)$ th rotor flux can be calculated from the current model of IM as [6], [14]

$$\psi_r^{k+2} = \psi_r^{k+1} + T_{sc} \left(R_r \frac{L_m}{L_r} i_s^{k+1} - \left(\frac{R_r}{L_r} - j\omega_r \right) \psi_r^{k+1} \right). \quad (16)$$

Based on the predicted value of ψ_r^{k+2} in (16), the phase angle of ψ_s^{ref} at $(k + 2)$ th instant can be obtained as

$$\angle \psi_s^{\text{ref}} = \angle \psi_r^{k+2} + \arcsin \left(\frac{T_e^{\text{ref}}}{\frac{3}{2} p \lambda L_m |\psi_r^{k+2}| |\psi_s^{\text{ref}}|} \right). \quad (17)$$

The final stator flux vector reference ψ_s^{ref} , which is equivalent to the original stator flux amplitude reference and torque reference in conventional MPTC, can be calculated from (13) and (17). After that, a cost function J_1 similar to (9) can be built to force stator flux ψ_s to track its reference, which is expressed as

$$J_1 = |\psi_s^{\text{ref}} - \psi_s^{k+2}|. \quad (18)$$

It is evident no weighing factor is required in (18). The prediction of stator flux at $(k + 2)$ th is obtained as follows:

$$\psi_s^{k+2} = \psi_s^{k+1} + (\mathbf{u}_s^{k+1} - R_s i_s^{k+1}) T_{sc} \quad (19)$$

where ψ_s^{k+1} and i_s^{k+1} are predicted from (4) to compensate the influence of one-step delay. Similar to vector selection described in Section III-B, the optimal voltage vector is determined by evaluating the cost function J_1 for each voltage vector and the one minimizing (18) is selected.

The process of the proposed MPFC can be summarized as follows.

- 1) Measure stator current, dc-link voltage, and rotor speed at k th instant.
- 2) Estimate stator flux $\hat{\psi}_s^k$ from (6) and predict i_s^{k+1} and ψ_s^{k+1} from (4) with $\hat{\psi}_s^k$ and i_s^k as initial states.
- 3) Predict ψ_r^{k+2} from (15) and (16), ψ_s^{k+2} from (19), and then calculate the desired phase angle of ψ_s^{ref} using (17).
- 4) Calculate the final new stator flux vector reference according to (13) and substitute it into (18) to select the best voltage vector minimizing (18).

B. Improved MPFC With Switching Instant Optimization

As can be seen in (18), the weighting factor for stator flux is avoided by transforming the references of torque and stator flux magnitude into an equivalent reference of stator flux vector. This helps to save much offline tuning work and significantly improves the practicability of MPFC. However, similar to the conventional MPTC, applying the selected voltage vector during the whole control period will still bring considerable torque ripple and current harmonics [9], [14].

In the improved MPFC, the switching instant of the selected vector will be optimized to further improve the steady-state per-

formance of the proposed scheme. Different from prior MPTC with duty cycle control [9], [14], which applies the selected voltage vector at the beginning of the next control period, the old voltage vector applied during the last period will be applied first in the proposed MPFC, followed by the selected voltage vector. The stator flux at the end of next control period can be expressed as

$$\psi_s^{k+2} = \psi_s^{k+1} + \mathbf{f}_{\text{old}}^k t_{\text{opt}} + \mathbf{f}_i^{k+1} (T_{sc} - t_{\text{opt}}) \quad (20)$$

where \mathbf{f}_{old} and \mathbf{f}_i^{k+1} ($i \in \{0, 1, \dots, 7\}$) are the stator flux slopes for voltage vector \mathbf{u}_{old} applied at previous period and a selected voltage vector \mathbf{u}_{si}^{k+1} , respectively. t_{opt} is the optimal duration for \mathbf{u}_{old} . Within a short control period, the stator flux slope for \mathbf{u}_{si}^{k+1} can be assumed constant and it is calculated as follows:

$$\mathbf{f}_i^{k+1} = \frac{d\psi_{si}}{dt} = \mathbf{u}_{si}^{k+1} - R_s i_s^{k+1}. \quad (21)$$

Substituting (20) into (18), the cost function can be considered as a function of t_{opt} , namely $J_1 = J_1(t_{\text{opt}})$. Minimizing (18) is equivalent to solving the following equation:

$$\frac{\partial J_1(t_{\text{opt}})}{\partial t_{\text{opt}}} = 0. \quad (22)$$

Combining (20) to (22), the optimal switching instant is finally derived as

$$t_{\text{opt}} = \frac{(\psi_s^{\text{ref}} - \psi_s^{k+1} - \mathbf{f}_i^{k+1} T_{sc}) \odot (\mathbf{f}_{\text{old}} - \mathbf{f}_i^{k+1})}{|\mathbf{f}_{\text{old}} - \mathbf{f}_i^{k+1}|^2} \quad (23)$$

where \odot represents the dot product of two complex vectors. In the practical application, t_{opt} is limited in the range of $[0, T_{sc}]$ for the aim of protection.

For two-level inverter-fed IM drives, the optimal switching instant t_{opt} is calculated for each feasible voltage vector \mathbf{u}_{si}^{k+1} ($i \in \{0, 1, \dots, 7\}$) according to (23). After the optimal switching time t_{opt} is determined for a given voltage vector \mathbf{u}_{si}^{k+1} , stator flux at $(k + 2)$ th instant can be predicted as

$$\psi_{si}^{k+2} = \psi_s^{k+1} + (\mathbf{u}_{\text{old}} - \mathbf{u}_{si}^{k+1}) t_i + (\mathbf{u}_{si}^{k+1} - R_s i_s) T_{sc}. \quad (24)$$

The value of ψ_{si}^{k+2} is subsequently evaluated by the cost function presented in (18) to determine the best voltage vector and its optimal duration.

With the procedures above, the minimal tracking error of stator flux vector can be achieved at the end of next control period. However, high deviation of stator flux at the switching instant may occur. This can be illustrated by the two possible stator flux trajectories shown in Fig. 3. It can be seen that, although both stator flux trajectories (represented as a and b in Fig. 3) can reach the stator flux vector reference at the end of control period, the trajectory a is preferred because it is more smooth and has smaller deviation from the reference vector during the whole control period. To prevent high deviation of stator flux during the control period, a penalty on deviation at the switching instant is added in cost function (18), namely

$$J_2 = |\psi_s^{\text{ref}} - \psi_s^{k+2}| + |\psi_s^{\text{ref}} - \psi_s^t| \quad (25)$$

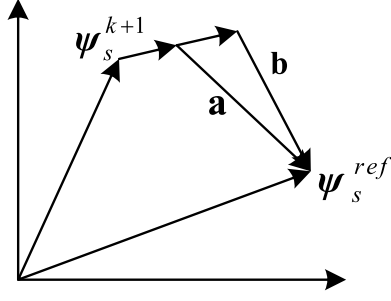


Fig. 3. Two trajectories of stator flux during one control period.

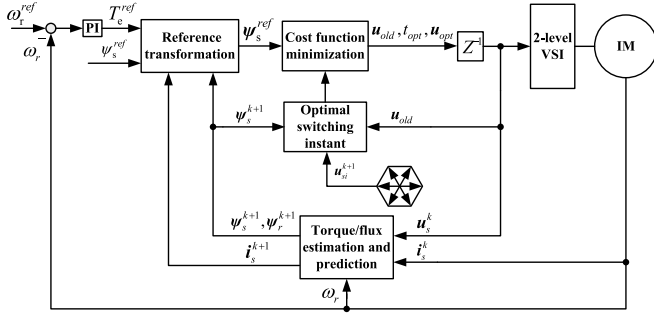


Fig. 4. Control diagram of proposed MPTC with switching instant optimization.

 TABLE I
 MACHINE AND CONTROL PARAMETERS

DC-bus voltage	U_{dc}	540 V
Rated power	P_N	2.2 kW
Rated voltage	U_N	380 V
Rated frequency	f_N	50 Hz
Number of pole pairs	N_p	2
Stator resistance	R_s	3.126 Ω
Rotor resistance	R_r	1.879 Ω
Mutual inductance	L_m	0.221 H
Stator inductance	L_s	0.230 H
Rotor inductance	L_r	0.230 H
Sampling period	T_{sc}	50 μ s
Flux amplitude reference	$ \psi_s^* $	0.91 Wb

where stator flux vector ψ_s^t is the stator flux vector at the optimal switching instant and it can be obtained as follows:

$$\psi_s^t = \psi_s^{k+1} + \mathbf{u}_{old} t_i. \quad (26)$$

Hence, after $\psi_{s_i}^{k+2}$ and ψ_s^t are obtained from (24) and (26) for a given voltage vector $\mathbf{u}_{s_i}^{k+1}$, they are subsequently evaluated by the cost function presented in (25). After all the voltage vectors together with their optimal switching instants are evaluated with the cost function (25), the best voltage vector \mathbf{u}_{opt} with its optimal switching instant t_{opt} minimizing (25) is selected and applied in the next control period.

The overall control diagram of proposed MPFC is shown in Fig. 4.

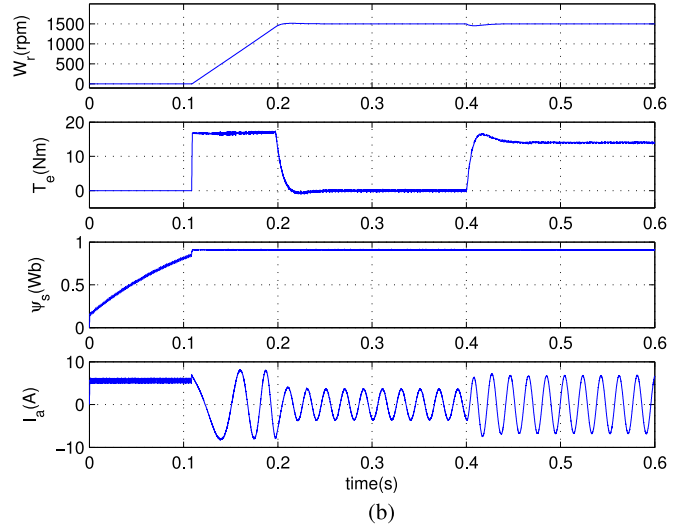
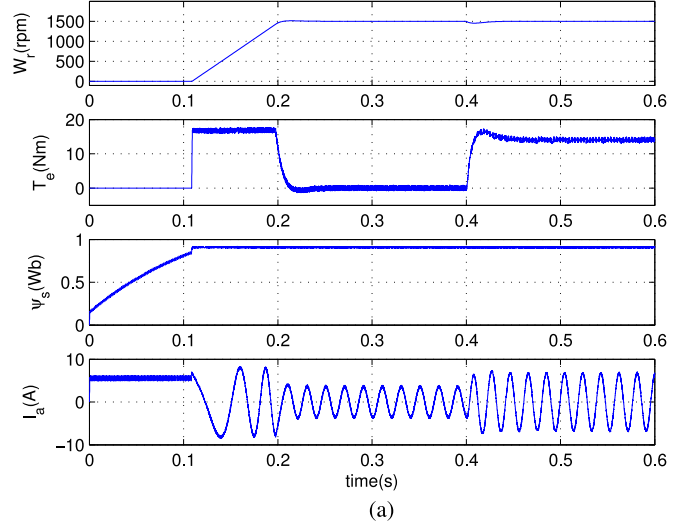


Fig. 5. Simulated starting responses from standstill to 1500 r/min for (a) method I and (b) method II.

V. SIMULATION AND EXPERIMENTAL RESULTS

A. Simulation Results

The proposed MPFC is simulated in the environment of MATLAB/Simulink to validate its effectiveness. The machine and control parameters are listed in Table I. For convenience, the basic MPFC without flux weighting factor is referred as method I and the improved MPTC with switching instant optimization is referred as method II in the following text, respectively.

Fig. 5 shows the starting responses from standstill to 1500 r/min for both methods. The stator flux is first established using preexcitation, and during the accelerating stage, the torque is limited to 120% rated value (16.8 N · m). At $t = 0.4$ s, an external load with rated value (14 N · m) is suddenly applied to the machine. From top to bottom, the curves shown in Fig. 5 are speed, torque, stator flux, and stator current, respectively. It is clearly seen that the proposed MPTC works well over a wide speed range and exhibits strong robustness against load disturbance. Similar dynamic responses can be observed in method II, but it presents much lower torque and flux ripples.

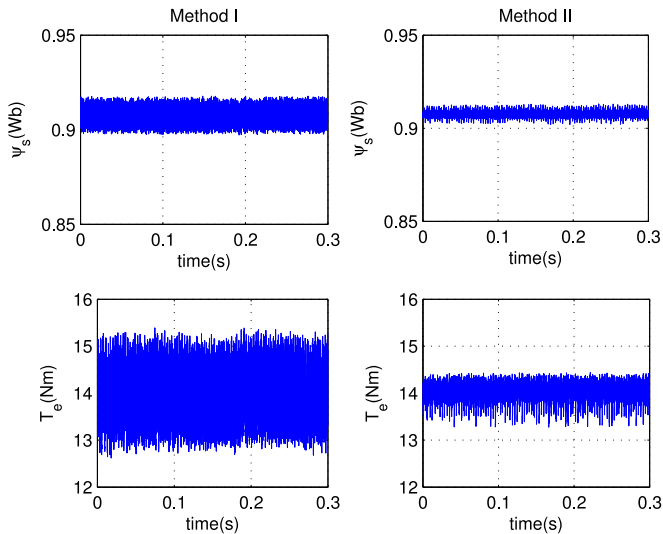


Fig. 6. Simulated steady-state response at 1500 r/min for (a) method I and (b) method II.

A more detailed steady-state waveforms of torque and stator flux with 100% rated torque are demonstrated in Fig. 6. It is seen that both torque and flux ripples in method II are much lower than those in method I, confirming the effectiveness of the method II with switching instant optimization.

To illustrate the influence of machine parameter variations on the performance of system, Fig. 7 shows the simulated responses of method II at low and high speeds when the stator and rotor resistances are increased by 50% and 100%, respectively. It is seen that the system works well at both low and high speeds, even if the stator and rotor resistances vary significantly from its actual value. The current is very sinusoidal in shape. As a closed-loop full-order observer is employed, only very minor tracking error of stator flux can be observed in low-speed operation and the flux error at high speed is negligible. The simulation results prove that the proposed method has some robustness against machine parameter variations.

B. Experimental Results

The experimental tests were carried out on a two-level inverter-fed IM drive platform to further validate the effectiveness of the proposed method. A 32-bit floating point digital signal processor TMS320F28335 is employed to accomplish the developed control algorithm. The control and system parameters are the same as those listed in Table I. The overall control diagram has been presented in Fig. 4. The tested maximum execution time including AD sampling, communication, observer, and the control algorithm is $34.8 \mu\text{s}$, which is well below the sampling period of $50 \mu\text{s}$. Hence, it is sufficient to accomplish all the functions within each sampling period. In the following tests, all variables are displayed on digital oscilloscope via on-board DA converter except the stator current, which is measured directly by a current probe.

First, the steady-state performance at low and high speeds is investigated. The tests with rated load torque at both low and high speeds are presented in Figs. 8 and 9, respectively.

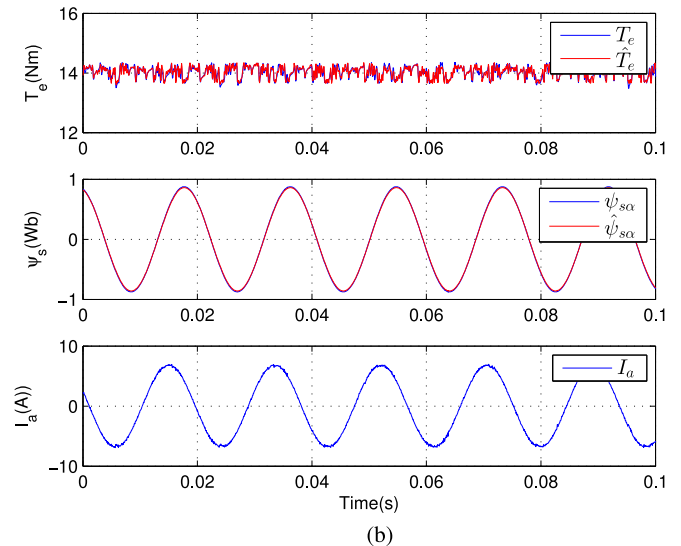
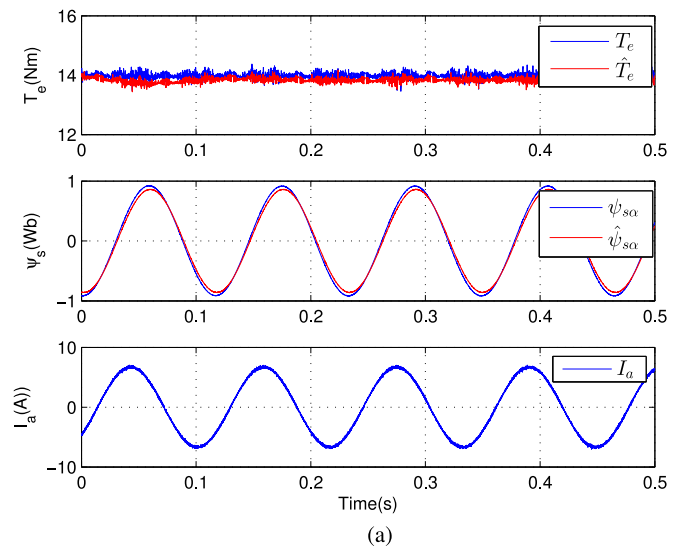


Fig. 7. Simulated responses of method II with mismatched machine parameters. (a) Both the stator and rotor resistances are increased by 50% at 150 r/min. (b) Both the stator and rotor resistances are increased by 100% at 1500 r/min.

It is seen that the proposed MPTC is stable and works well at both low and high speeds. Similar to the responses without load, method II exhibits much lower torque/flux ripples and the stator current is more sinusoidal in shape with much less harmonics than method I. It should be noted that there are some insignificant spikes in the measured speed, which are mainly caused by the speed measurement and DA conversion. In fact, the motor runs steadily and the real speed is smooth, which can be confirmed by the sinusoidal stator current measured directly by a current probe. These experimental results validate that the proposed MPTC performs well at both low and high speeds with or without load.

Apart from steady-state tests, the dynamic responses and robustness against load disturbance were also carried out. Fig. 10 presents the starting response from standstill to 1500 r/min without load. From top to bottom, the curves shown in Fig. 10 are rotor speed, electromagnetic torque, stator flux, and stator current.

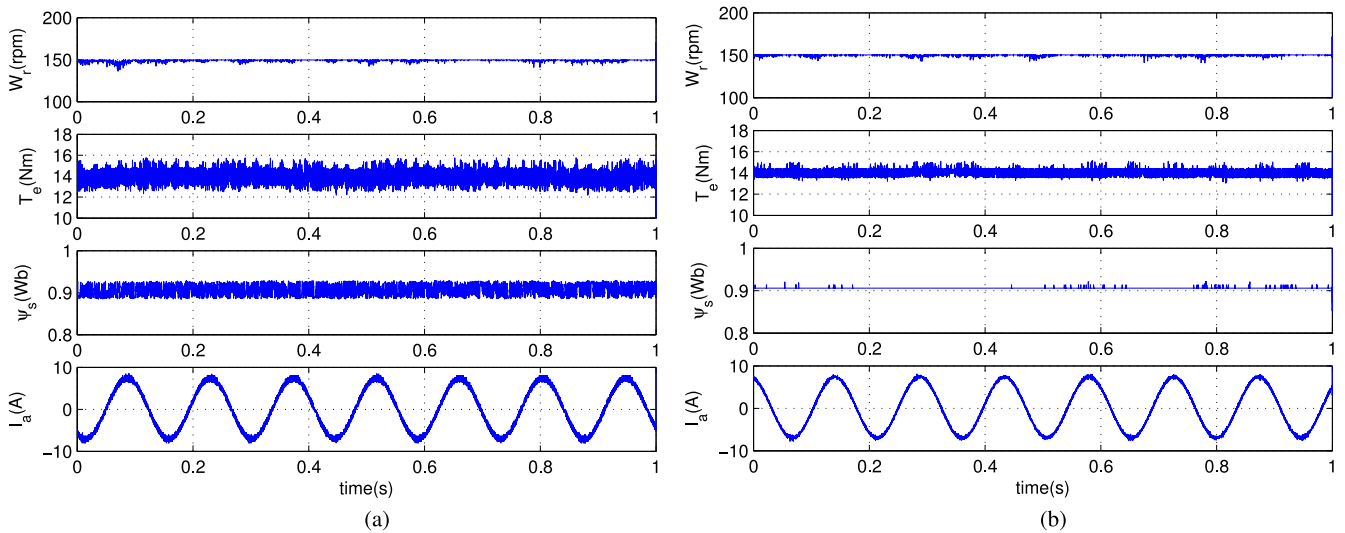


Fig. 8. Measured low-speed operation of 150 r/min with rated torque for (a) method I and (b) method II.

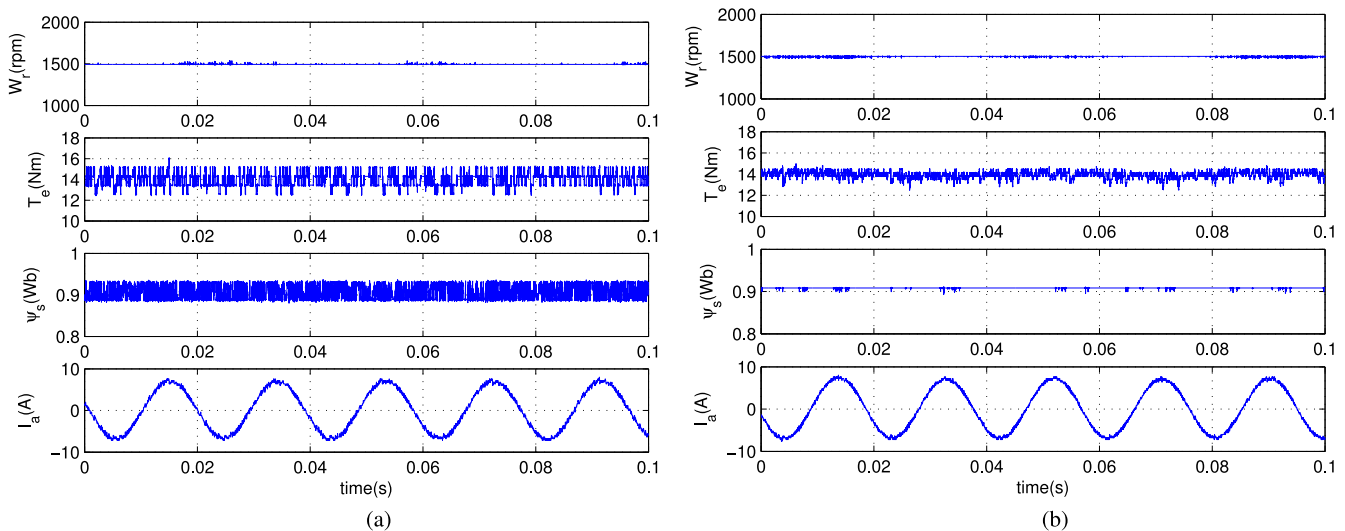


Fig. 9. Measured high-speed operation of 1500 r/min with rated torque for (a) method I and (b) method II.

As the stator current is not directly controlled in the proposed method, to prevent large current during start-up process, the stator flux is first established before starting the motor. Otherwise, the starting current would be very large, which is harmful to the inverters, as shown in [2] and [6]. It is seen that the motor accelerates quickly to 1500 r/min without large start-up current after the process of preexcitation. Much lower torque and flux ripples can be observed in method II. During the dynamic process, decoupled control of torque and stator flux is achieved in both methods. This proves that, by using the new stator flux vector reference, the fast and accurate control of torque and stator flux can be realized. Meanwhile, the weighting factor tuning effort required in the conventional MPTC is eliminated.

The responses to external load disturbance is shown in Fig. 11, where an external load of $14 \text{ N} \cdot \text{m}$ (100% rated torque) is suddenly applied to the machine. It can be seen that the speed re-

turns to its reference quickly after a small speed drop, exhibiting strong robustness against external load disturbance. The stator flux is not affected by the stepped change of torque, and method II still exhibits lower torque and flux ripples.

Furthermore, the responses during speed reversals are shown in Fig. 12. It can be seen that the motor accelerates quickly from -1500 to 1500 r/min. The flux magnitudes of both methods keep constant during the dynamic process, indicating that decoupled control of stator flux and torque is realized while eliminating the use of weighting factor. The dynamic responses of both methods are similar, but method II is evidently superior to method I in terms of torque, flux, and current ripples.

Finally, the average switching frequency during steady-state operating at different speeds was investigated. The results are shown in Fig. 13. It is seen that the switching frequency of the method II is almost constant during various operating conditions

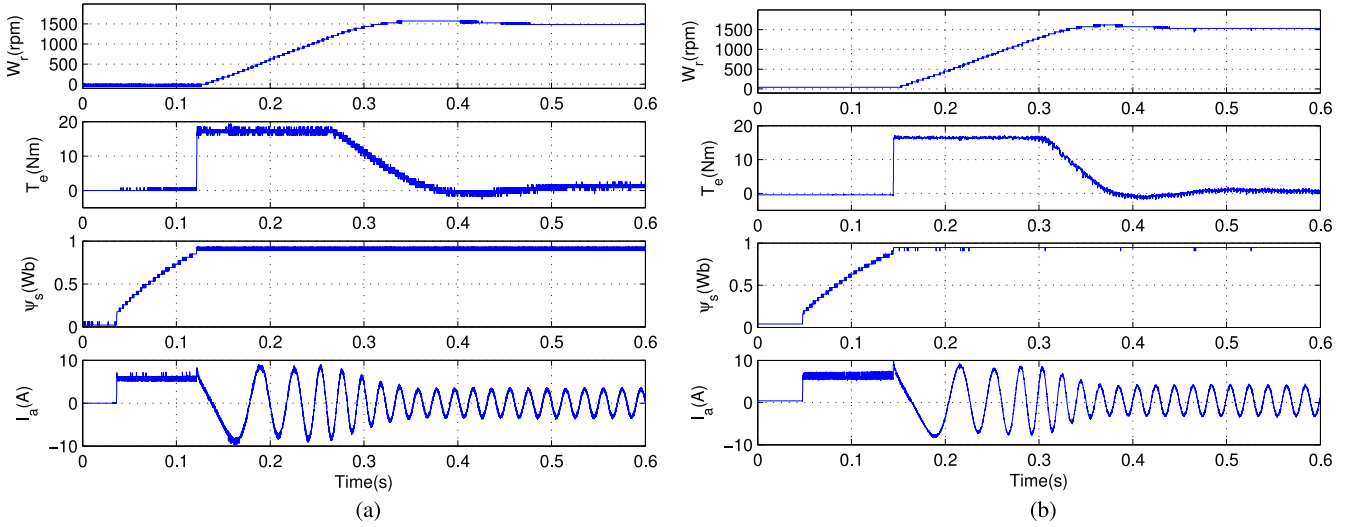


Fig. 10. Measured starting responses from standstill to 1500 r/min for (a) method I and (b) method II.

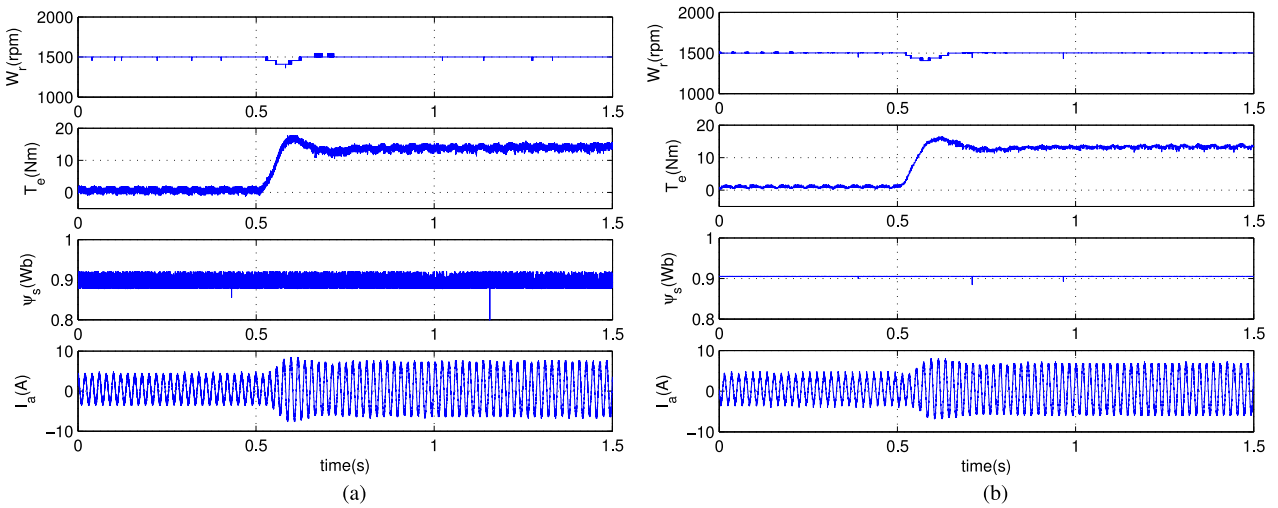


Fig. 11. Measured responses to 100% rated load disturbance for (a) method I and (b) method II.

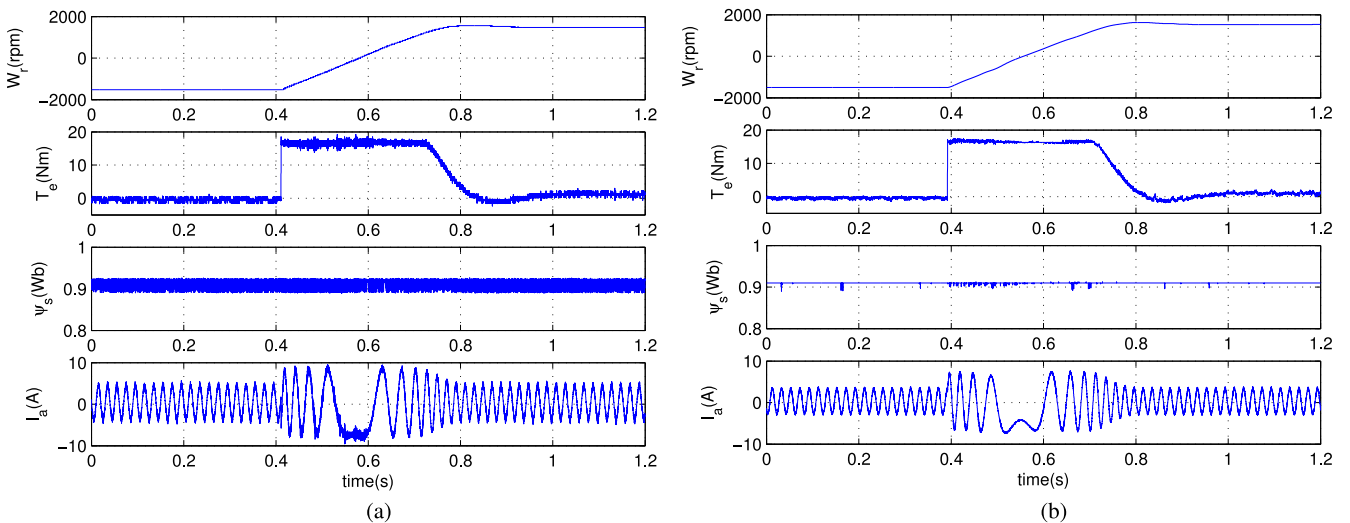


Fig. 12. Measured responses of speed reversal at 1500 r/min for (a) method I and (b) method II.

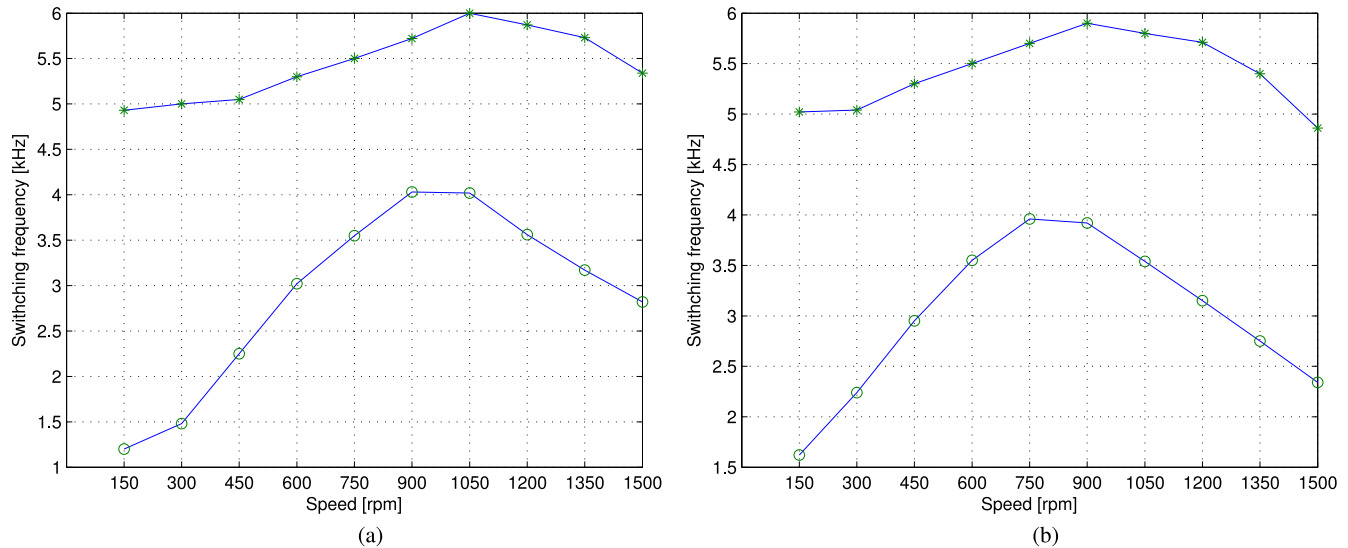


Fig. 13. Measured average switching frequency of method I (marked with “o”) and method II (marked with “*”). (a) Without load. (b) With rated load.

and higher than that of method I. This indicates that method II is more suitable for applications requiring higher steady-state performance, while method I is more favorable for applications concerning on low switching frequency.

VI. CONCLUSION

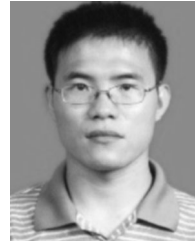
Conventional MPTC suffers from the problems of weighting factor tuning for stator flux and relatively high torque ripples at steady state. This paper proposes an MPFC without weighting factor for two-level inverter-fed IM drives. By investigating the inherent relationship between stator flux and torque based on IM model, a new stator flux vector reference is equivalently obtained from original references of torque and stator flux amplitude. Thus, simultaneous control of both torque and stator flux in conventional MPTC is replaced by control of a stator flux vector and the weighting factor tuning is eliminated. Two variants of MPFC are proposed in this paper, with the first one focusing on low switching frequency while the second one concerning more on the steady-state performance by introducing switching instant optimization.

Both simulation and experimental results prove that the proposed MPTC performs well over a wide speed range with or without load. Decoupled control of torque and stator flux is achieved during both steady-state operation and dynamic process. By introducing the switching instant optimization, much better steady-state performance in terms of torque/flux ripples and current harmonics can be observed, without affecting the dynamic responses. The proposed MPFC improves the practicability of conventional MPTC significantly.

REFERENCES

- [1] D. Casadei, F. Profumo, G. Serra, and A. Tani, “FOC and DTC: Two viable schemes for induction motors torque control,” *IEEE Trans. Power Electron.*, vol. 17, no. 5, pp. 779–787, Sep. 2002.
- [2] Y. Zhang, J. Zhu, Z. Zhao, W. Xu, and D. Dorrell, “An improved direct torque control for three-level inverter-fed induction motor sensorless drive,” *IEEE Trans. Power Electron.*, vol. 27, no. 3, pp. 1502–1513, Mar. 2012.
- [3] G. S. Buja and M. P. Kazmierkowski, “Direct torque control of PWM inverter-fed AC motors—A survey,” *IEEE Trans. Ind. Electron.*, vol. 51, no. 4, pp. 744–757, Aug. 2004.
- [4] N. Hur, K. Nam, and S. Won, “A two-degrees-of-freedom current control scheme for deadtime compensation,” *IEEE Trans. Ind. Electron.*, vol. 47, no. 3, pp. 557–564, Jun. 2000.
- [5] J.-K. Kang and S.-K. Sul, “New direct torque control of induction motor for minimum torque ripple and constant switching frequency,” *IEEE Trans. Ind. Appl.*, vol. 35, no. 5, pp. 1076–1082, Sep./Oct. 1999.
- [6] H. Miranda, P. Cortes, J. I. Yuz, and J. Rodriguez, “Predictive torque control of induction machines based on state-space models,” *IEEE Trans. Ind. Electron.*, vol. 56, no. 6, pp. 1916–1924, Jun. 2009.
- [7] J. Rodriguez and P. Cortes, *Predictive Control of Power Converters and Electrical Drives*. Hoboken, NJ, USA: Wiley-IEEE Press, 2012.
- [8] C. A. Rojas, J. Rodriguez, F. Villarroel, J. R. Espinoza, C. A. Silva, and M. Trincado, “Predictive torque and flux control without weighting factors,” *IEEE Trans. Ind. Electron.*, vol. 60, no. 2, pp. 681–690, Feb. 2013.
- [9] S. A. Davari, D. A. Khaburi, and R. Kennel, “An improved FCS-MPC algorithm for an induction motor with an imposed optimized weighting factor,” *IEEE Trans. Power Electron.*, vol. 27, no. 3, pp. 1540–1551, Mar. 2012.
- [10] Y. Zhang and H. Yang, “Generalized two-vector-based model-predictive torque control of induction motor drives,” *IEEE Trans. Power Electron.*, vol. 30, no. 7, pp. 3818–3829, Jul. 2015.
- [11] S. Mariethoz, A. Domahidi, and M. Morari, “High-bandwidth explicit model predictive control of electrical drives,” *IEEE Trans. Ind. Appl.*, vol. 48, no. 6, pp. 1980–1992, Nov./Dec. 2012.
- [12] T. Geyer, G. Papafotiou, and M. Morari, “Model predictive direct torque control—Part I: Concept, algorithm, and analysis,” *IEEE Trans. Ind. Electron.*, vol. 56, no. 6, pp. 1894–1905, Jun. 2009.
- [13] F. Villarroel, J. R. Espinoza, C. A. Rojas, J. Rodriguez, M. Rivera, and D. Sbarbaro, “Multiobjective switching state selector for finite-states model predictive control based on fuzzy decision making in a matrix converter,” *IEEE Trans. Ind. Electron.*, vol. 60, no. 2, pp. 589–599, Feb. 2013.
- [14] Y. Zhang and H. Yang, “Model predictive torque control of induction motor drives with optimal duty cycle control,” *IEEE Trans. Power Electron.*, vol. 29, no. 12, pp. 6593–6603, Dec. 2014.
- [15] P. Karamanakos, P. Stolze, R. M. Kennel, S. Manias, and H. du T. Mouton, “Variable switching point predictive torque control of induction machines,” *IEEE J. Emerging Sel. Topics Power Electron.*, vol. 2, no. 2, pp. 285–295, Jun. 2014.

- [16] N. Oikonomou and J. Holtz, "Stator flux trajectory tracking control for high-performance drives," in *Proc. 41st IAS Annu. Meeting Ind. Appl. Conf. Rec.*, 2006, vol. 3, pp. 1268–1275.
- [17] N. Oikonomou, C. Gutscher, P. Karamanakos, F. Kieferndorf, and T. Geyer, "Model predictive pulse pattern control for the five-level active neutral-point-clamped inverter," *IEEE Trans. Ind. Appl.*, vol. 49, no. 6, pp. 2583–2592, Nov./Dec. 2013.
- [18] J. Holtz, "The representation of ac machine dynamics by complex signal flow graphs," *IEEE Trans. Ind. Electron.*, vol. 42, no. 3, pp. 263–271, Jun. 1995.
- [19] L.-J. Diao, D. N. Sun, K. Dong, L.-T. Zhao, and Z.-G. Liu, "Optimized design of discrete traction induction motor model at low-switching frequency," *IEEE Trans. Power Electron.*, vol. 28, no. 10, pp. 4803–4810, Oct. 2013.
- [20] Q. Li, N. Wang, and D. Yi, *Numerical Analysis*. Hsinchu, Taiwan: Tsinghua Univ. Press, 2001.
- [21] Z. Yongchang and Z. Zhengming, "Speed sensorless control for three-level inverter-fed induction motors using an extended Luenberger observer," in *Proc. Vehicle Power Propulsion Conf.*, 2008, pp. 1–5.
- [22] P. Cortes, J. Rodriguez, C. Silva, and A. Flores, "Delay compensation in model predictive current control of a three-phase inverter," *IEEE Trans. Ind. Electron.*, vol. 59, no. 2, pp. 1323–1325, Feb. 2012.
- [23] J. Rodriguez, R. M. Kennel, J. R. Espinoza, M. Trincado, C. A. Silva, and C. A. Rojas, "High-performance control strategies for electrical drives: An experimental assessment," *IEEE Trans. Ind. Electron.*, vol. 59, no. 2, pp. 812–820, Feb. 2012.



Yongchang Zhang (M'10) received the B.S. degree from Chongqing University, Chongqing, China, in 2004, and the Ph.D. degree from Tsinghua University, Beijing, China, in 2009, both in electrical engineering.

From August 2009 to August 2011, he was a Post-doctoral Fellow with the University of Technology, Sydney, Australia. He joined the North China University of Technology, Beijing, in August 2011, as an Associate Professor. He is currently a Full Professor and the Vice Director of the Inverter Technologies Engineering Research Center of Beijing, Beijing. He has published more than 100 technical papers in the area of motor drives, pulse-width modulation, and ac/dc converters. His current research interests include model-predictive control for power converters and motor drives.



Haitao Yang (S'14) was born in 1987. He received the B.S. degree in electrical engineering from the Hefei University of Technology, Hefei, China, in 2009. He is currently working toward the Master's degree in electrical engineering at the North China University of Technology, Beijing, China.

His research interests include model-predictive control of motor drives.